Journal of Alloys and Compounds 574 (2013) 131–135

Contents lists available at SciVerse ScienceDirect

Journal of Alloys and Compounds

journal homepage: www.elsevier.com/locate/jalcom

Synthesis and size dependent exchange bias effect in $CoCr_2O_4/Cr_2O_3$ nanogranular systems

Zhaoming Tian [a,*], Shuai Huang [a], Songliu Yuan [a,b], Junfeng Wang [b]

[a] School of Physics, Huazhong University of Science and Technology, Wuhan, PR China
[b] Wuhan Pulsed High Magnetic Field Center, Huazhong University of Science and Technology, Wuhan 430074, PR China

ARTICLE INFO

Article history:
Received 5 December 2012
Received in revised form 25 March 2013
Accepted 31 March 2013
Available online 18 April 2013

Keywords:
Exchange bias
Antiferromagnetic

ABSTRACT

Structure and magnetic properties have been investigated on the nanogranular systems of ferrimagnetic (Ferri) $CoCr_2O_4$ nanoparticles embedded in antiferromagnetic (AFM) Cr_2O_3 matrix, synthesized by a phase segregation route from diluted $Cr_{2(1-x)}Co_{2x}O_3$ ($x = 0.1$) oxides. The $CoCr_2O_4$ nanoparticles with average particle size (D_{CCO}) from 8 to 60 nm can be produced by varying synthesis temperatures. Magnetization measurement show that, both exchange bias fields (H_{EB}) and vertical magnetization shift (M_{Shift}) can be found at 10 K after field-cooled from 350 K. With increasing particle size (D_{CCO}), both H_{EB} and M_{Shift} decrease monotonically and finally disappear as particle size is above 60 nm. The linear relationship between H_{EB} and M_{Shift} indicates that the interfacial frozen uncompensated spins play a critical role in inducing exchange bias effect.

© 2013 Elsevier B.V. All rights reserved.

1. Introduction

In past decades, nanocomposites have received much attention owing to the synergistic properties induced by the interactions between different nanometer-scale objects. They could show fascinating magnetic, magnetoelectric, and magneto-optical properties that can be tuned by the interfacial interactions between the different nanocomposites [1–3]. This provides a new opportunity to develop multifunctional nanomaterials for applications in plenty of fields, especially in biomedical, spintronic, and energy related areas [3].

When the nanocomposites are comprised by the ferromagnetic (FM) and antiferromagnetic (AFM) phases, an interesting proximity effect can occur, for example, the exchange bias (EB) effect [4,5]. Such an EB effect is originated from the exchange coupling between FM and AFM phases at interfaces, the main feature is that the shift of hysteresis loop along the magnetic field axis after the system field cooling through the Néel temperature of the antiferromagnet. Recently, EB effect in the FM/AFM nanostructures are acquiring attention, because the interface exchange coupling can be useful to overcome the superparamagnetic limit and increase the thermoremanence of FM nanoparticles [6], a critical bottleneck for magnetic data storage application. While, much attentions have been paid on exchange-coupled nanosystems of transition metal particles embedded in their native oxides, such as Co–CoO [7], Ni–NiO [8], and Fe–Fe_xO_y [9], or oxides with different oxidation states, as in CrO_2–Cr_2O_3 [10], Fe_3O_4–FeO [11], and Mn_3O_4–MnO [12]. These restrict the technological applications of these types of materials. Thus, the strategy to fabricate complex FM–AFM nanostructures from alternative materials other than partially oxided metal nanoparticles, is of paramount interest.

Another important issue in FM–AFM nanocomposites is the finite-size scaling behavior. As the dimensions of the nanostructures reduce down to the nanometer scale, surface and interface effects become more important owing to the large surface atoms/bulk atoms ratio. Some of the basic magnetic properties become strongly size dependent, an enhancement of the coercive field (H_C) or the asymmetry of the hysteresis loops can be observed. However, size scaling on EB effect is still a controversial subject. Some authors reported that EB fields (H_{EB}) were enhanced with size reduction of FM component in FM/AFM heterostructures [13–15], whereas others observed the opposite trend [11,16]. These discrepancies have been attributed to different factors which impact the interfacial coupling, such as interfacial roughness, chemical nonstoichiometry, residual stress and grain shapes [13–17], a full understanding of this phenomenon still remains elusive. In addition, most studies are focused on the film systems, size-scaling of EB effect in granular systems that confines FM nanoparticles to AFM matrix is less investigated.

Based on above consideration, the motivation of this work is to fabricate bimagnetic AFM/ferrimagnetic (Ferri) nanostructures and investigate size scaling behavior of EB effect. A series of nanogranular systems of Ferri $CoCr_2O_4$ nanoparticles with different average particle size embedded in an AFM Cr_2O_3 matrix have been

* Corresponding author. Tel.: +86 18995621009.
E-mail addresses: tianzhaoming@mail.hust.edu.cn (Z. Tian), yuansl@hust.edu.cn (S. Yuan).

0925-8388/$ - see front matter © 2013 Elsevier B.V. All rights reserved.
http://dx.doi.org/10.1016/j.jallcom.2013.03.285

synthesized via a phase segregation route from Co-doped Cr_2O_3 oxides. Both EB fields (H_{EB}) and vertical magnetization shift (M_{Shift}) can be exhibited in these systems, and the magnitude of H_{EB} can be tailored by varying particle sizes.

2. Experimental

The $CoCr_2O_4/Cr_2O_3$ nanogranular systems have been prepared by a phase segregation route from diluted $Cr_{2(1-x)}Co_{2x}O_3$ ($x = 0.1$) oxides, as described below. High-pure chromium nitrate ($Cr(NO_3)_3{\cdot}9H_2O$), cobalfous nitrate ($Co(NO_3)_2{\cdot}6H_2O$), and ammonium bicarbonate (NH_4HCO_3) were employed as the starting raw materials. Stoichiometric amounts of chromium nitrate ($Cr(NO_3)_3{\cdot}9H_2O$) and cobalfous nitrate ($Co(NO_3)_2{\cdot}6H_2O$) were dissolved in distilled water. Subsequently, the upper mixture solution was slowly poured into the excessive ammonium bicarbonate (NH_4HCO_3) solution under constant stirring. After that, the resulting precipitation was washed and dried in air at 300 °C to obtain precursor powders. Finally, in order to fabricate the $Cr_2O_3/CoCr_2O_4$ nanocomposites with different particle sizes, the obtained precursor powders were sintered at different temperatures (T_s) from 600 °C to 1100°C for 3 h.

The crystal structure of the sintered samples was measured by X-ray diffraction (XRD, Philips X'pert pro). The micrographs of $CoCr_2O_4/Cr_2O_3$ nanogranular system were investigated by field emission scanning electron microscopy (FE-SEM) and transmission electron microscopy (TEM). The magnetic properties were performed using a commercial physical properties measurements system (PPMS, quantum design).

3. Results and discussion

Fig. 1 shows the X-ray diffraction (XRD) patterns for the $Cr_{2(1-x)}Co_{2x}O_3$ ($x = 0.1$) oxides sintered at different temperatures. For sample sintered at 600 °C, all diffraction peaks can be indexed to rhombohedral Cr_2O_3 phase, no impurity phases are detected within the XRD resolution, indicates that $CoCr_2O_4$ nanoparticles have not been precipitated from the diluted $Cr_{2(1-x)}Co_{2x}O_3$ ($x = 0.1$) oxides. As sintering temperature increases to 700 °C, typical (220), (311), (400), and (511) diffraction peaks corresponding to $CoCr_2O_4$ phases can be observed, reveals the coexistence of Ferri $CoCr_2O_4$ and AFM Cr_2O_3 phases. Moreover, the diffraction peaks become intensive and narrowing as sintering temperature increases due to their particle size growth. As for the formation of these binary-phase nanogranular system, we argue that part of Co cations are reacted with Cr cations to form Ferri $CoCr_2O_4$ phase during high temperature thermal treatment, leaving the other Cr_2O_3 as the AFM phase. That means that, Co-doped Cr_2O_3 oxides have phase separated into Ferri

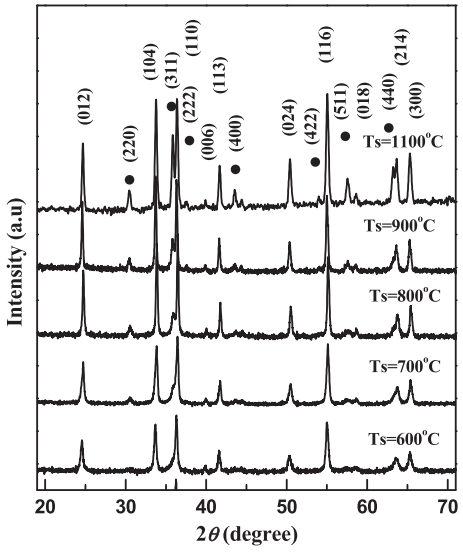

Fig. 1. The XRD patterns of $CoCr_2O_4/Cr_2O_3$ nanogranular systems sintered at different temperatures from 600 °C to 1100 °C, respectively. The (●) indicate these corresponding peaks from $CoCr_2O_4$.

$CoCr_2O_4$ and AFM Cr_2O_3 phases by a local arrangement of the Co and Cr cations during thermal treated at higher temperatures ($T_s \geqslant 700$ °C). Similar phenomenon has recently been observed in diluted $Ge_{1-x}Mn_xTe$ semiconductors [18], where MnTe is phase separated from the Mn-doped GeTe compound driven by the non-uniform Mn distribution produced at high thermal treatment.

The morphology and size of the serial of $CoCr_2O_4/Cr_2O_3$ nanocomposites are characterized by TEM, as shown in Fig. 2. Two-size distributed nanoparticles can be found for each sample from Fig. 2a–d. This means that a mixture of two discrete particles is resulted during thermal treatment at high temperatures. Combined with the XRD patterns, we can estimate that the smaller nanoparticles are $CoCr_2O_4$ phase, which are segregated to the edge of the Cr_2O_3 matrix or dispersed within the Cr_2O_3 particles. These results are consistent with the SEM analysis shown in Fig. 3, where smaller sized $CoCr_2O_4$ nanoparticles are well dispersed within the Cr_2O_3 matrix. In view of this point, each sample can be considered as a nanogranular system of Ferri $CoCr_2O_4$ nanoparticles embedded in AFM Cr_2O_3 matrix. Moreover, the particle size of $CoCr_2O_4$ phase can be tuned by varying synthesis temperature. By manually measuring the equivalent diameters of >50 particles from TEM micrographs, the average particle size of $CoCr_2O_4$ nanoparticles (D_{CCO}) is estimated to be about 8(±2) nm, 18(±3) nm, 30(±5) nm and 60(±5) nm for samples sintered at 700 °C, 800 °C, 900 °C and 1100 °C, respectively. The average particle size of $CoCr_2O_4$ follows a systematic behavior with synthesis temperature, in accordance with the crystalline sizes calculated by the Scherer formula from XRD spectrum. In contrast, the Cr_2O_3 particles grow slowly and have a broad size distribution. To obtain a more comprehensive picture of these binary composites, high resolution transmission electron micrograph (HRTEM) for sample sintered at 800 °C is shown in Fig. 2e and f, it reveals that $CoCr_2O_4$ nanoparticles have a diameter about 15–20 nm and Cr_2O_3 phases are in the range from 60 nm to 120 nm. Additionally, structural disorder region are existed at the $Cr_2O_3/CoCr_2O_4$ interface and the surface of $CoCr_2O_4$ nanoparticles. From the inset of Fig. 2f, the thickness is evaluated to be ~2.5 nm extended from the $CoCr_2O_4$ cores. This structural disorder layers can be correlated with the broken of chemical bond, chemical intermixing and amorphous structural defects at interfaces, as recent report in Ni/NiO and $NiFe_2O_4$ nanoparticles [19,20].

Temperature-dependent magnetizations in zero-field cooled (ZFC) and field cooled (FC) procedure under $H = 40$ kOe have been measured for the $CoCr_2O_4/Cr_2O_3$ nanogranular systems, as shown in Fig. 4. For all samples, FC magnetization curve shows an abrupt increase around 100 K marked the Ferri transition of $CoCr_2O_4$ phases, and there is an anomaly at $T_s \sim 26$ K associated with the spiral magnetic order of the $CoCr_2O_4$ phase, responsible for the onset of ferroelectricity as reported by Choi et al. [21]. Moreover, the ZFC and FC magnetization curves show distinct divergence below the irreversibility temperature T_{irr}, defined as the irreversible magnetization $\triangle M = M_{FC} - M_{ZFC}$ becomes different from zero. As particle size increases, this divergence becomes smaller, and ZFC and FC curves almost overlap when particle size (D_{CCO}) is above 60 nm. This irreversibility is associated with the freezing process of interfacial uncompensated spins as a consequence of strong exchange coupling across the Ferri/AFM interfaces, generally observed in spin disorder systems such as spin glassy and cluster glassy system [22,23]. The T_{irr} shift to lower temperature with increasing particle size reflects the weakening of interfacial coupling interaction.

Magnetic hysteresis loops are measured at 10 K after ZFC and FC process from 350 K with $H = 40$ kOe, as shown in Fig. 5. One can see that in the ZFC process the hysteresis loops display symmetric hysteresis loop around zero field, while in the FC case, the loops shift toward the negative field and the positive magnetization for samples with smaller particle size ($D_{CCO} \leqslant 30$ nm), indicative of the EB phenomena. Usually, the exchange field is defined as $H_{EB} = (H_{C1} + H_{C2})/2$

Download English Version:

https://daneshyari.com/en/article/1613557

Download Persian Version:

https://daneshyari.com/article/1613557

Daneshyari.com